

Research Article

Effect of Cold-Rolling and Annealing Treatments on the Microstructure and Mechanical Properties of AISI 309S Austenitic Stainless Steel

M. Eskandari*, I. Khosravi-Bigdeli, S.R. Alavi Zaree and M. Yeganeh

Department of Materials Science and Engineering, Faculty of Engineering, Shahid Chamran University of Ahvaz, Ahvaz, Iran

ARTICLE INFO

Article history:

Received 19 May 2022

Reviewed 11 June 2022

Revised 23 June 2022

Accepted 25 June 2022

Keywords:

Austenitic stainless steel

Annealing

Recrystallization

Mechanical property

ABSTRACT

Microstructural evolutions and mechanical properties of a cold-rolled 309S austenitic stainless steel were investigated after reversion annealing in the temperature ranges of 700-1000°C for 3-20 min. The specimen was first cold-rolled at room temperature to 90% thickness reduction. The microstructure was analyzed by optical and SEM methods and the mechanical behavior was studied by tensile tests and hardness measurement. The results depicted that negligible strain-induced α -martensite was formed after cold-rolling. In addition, elongated austenite grains were observed after deformation followed by annealing below 700°C which was a signature of the recovery process. The recrystallization of the deformed austenite was dominant above 800°C, while recrystallization followed by grain growth were seen at 900°C. Moreover, the significant grain growth was observed at 1000°C. The optimum annealing temperature and time for achievement of a uniform recrystallized grain were at 800°C for 3 min which resulted in considerable grain refinement. The grain refinement led to improvement of mechanical properties of investigated austenitic stainless steel. The hardness value of refined austenite grains was 195% greater than that of the as-received steel. Finally, current work can shed some light on the effect of grain refinement on the control of microstructural and mechanical property of austenitic stainless steels.

© Shiraz University, Shiraz, Iran, 2022

1. Introduction

Types 309 and 309S, which are chromium-nickel austenitic stainless steels, show excellent corrosion resistance. The 309S stainless steel has lower carbon content in comparison with the 309 steel that minimizes carbide precipitation and improves weldability [1, 2]. Such steels are widely used in furnace parts, aircraft, engine parts, heat exchangers, refineries, and chemical processing equipment. However, they possess low yield

strength (less than 150-200 MPa) which results in their unsuitability for structural applications [3]. As a result, different grain refining techniques, including cold-working accompanied by strain-induced martensitic transformation and annealing treatments, have been applied so far to strengthen austenitic stainless steels [4]. The cold-rolling and annealing treatments of austenitic stainless steels such as 304, 321, 301, 201, and 316L have been extensively reviewed in previous works [3, 5-8]. In the thermo-mechanical process, one of the

* Corresponding author

E-mail address: m.eskandari@scu.ac.ir (M. Eskandari)<https://doi.org/10.22099/IJMF.2022.43813.1228>

effective methods used to produce nanocrystalline stainless steel is the martensitic treatment [8-12]. It was reported that the strain-induced martensite formed during deformation in metastable austenitic stainless steels and martensite was reverted to austenite after subsequent annealing treatments resulted in significant grain refinement. Volume fraction of the martensite after deformation annealing time and temperature are one of the factors which the degree of grain refinement is dependent on. The influence of annealing time and temperature on the formation of reverted austenite grains in austenitic stainless steels after cold-rolling has been previously studied [9-11, 13].

On the other hand, some austenitic stainless steels are more resistant against martensitic transformation during cold-deformation. For instance, Lichtenfeld et al. [1] studied stress-strain curves of 309 and 304L stainless steels at room temperature. They observed that 304L steel depicted martensitic transformation readily with strain, while 309 steel did not exhibit strain-induced transformation. Hence, after cold deformation, it is expected that primary recrystallization is the main mechanism for grain refinement after annealing treatment in former steel. In addition to the recovery, recrystallization, and normal grain growth that occurs under different annealing times and temperatures, the abnormal grain growth (secondary recrystallization) also occurs in this state (different annealing times and temperatures) [5, 14]. To achieve a uniform fine-grained structure after cold rolling and annealing treatments, an optimum annealing condition should be obtained.

The recrystallization behavior in austenitic stainless steels has been investigated by several researchers [15-20]. Research by Donadille et al. [15] showed that at the location of the sites of shear bands, the nucleation of recrystallization occurred for 316L austenitic stainless steel. Yang et al. [16] investigated the cold-work in austenitic stainless steel and annealing behavior. The temperature for the initiation of recrystallization was found to be related to the stacking-fault energy (SFE). By conducting continuous recrystallization research on strain-induced fine grains of austenitic stainless steel, Belyakov et al. [17] found that annealing processes that

operated after large strain deformation were the cause of this recrystallization. Tihamiyu et al. [5] studied the microstructure of 321 austenitic stainless steel after cold rolling and annealing treatments in the temperature ranges of 650°C to 800°C to reach a structure with ultrafine grain. The martensite to austenite reversion along with recrystallization of primary austenite were identified as the main mechanisms for grain refinement of the austenite phase. They displayed that the optimum annealing temperature and time to achieve a fine-grained structure was 750°C for 10 min.

Examining the mechanical properties of the nanocrystalline 316L sample by Chen et al. [21], a high yield strength of up to 1450 MPa was reported, which follows the Hall-Petch relationship. The results were consistent with the experimental results of the previous studies, in other words, the hardness value of nanocrystalline iron samples with an average grain size of 6-60 nm follows the Hall-Petch relationship [22]. In addition, the results of the Shakhova [23] study on the yield stress of the plastic deformation method of Cr-Ni austenitic stainless steels and the grain size of this steel, show their dependence on each other (yield stress and grain size). Hence, it is essential to study annealing parameters (time and temperature) after cold-working to achieve uniform fine recrystallized grains. The present study aims to investigate microstructural evolutions and mechanical properties after annealing of a cold-rolled AISI 309S austenitic stainless steel to achieve an optimum annealing time and temperature.

2. Materials and Methods

A commercial AISI 309S austenitic stainless steel with the initial thickness of 6 mm was used. The chemical composition (wt.%) of investigated steel was listed in Table 1. The average grain size of the as-received material was around of $80 \pm 3 \mu\text{m}$.

Multi-pass unidirectional rolling was conducted at room temperature to achieve a 90% thickness reduction.

Table 1. Chemical composition of the investigated material

Element	C	Si	Mn	S	Cr	Ni	Fe
wt.%	0.062	0.46	1.03	<0.0002	22.6	13.4	Bal.

To avoid a temperature rise during the rolling, the sample was soaked after 4 passes into a mixture of water and ice during rolling to prevent adiabatic heating formation. Subsequently, the cold-rolled specimens were annealed at temperatures of 700°C, 800°C, 900°C to 1000°C for 3, 5, 10, and 20 min followed by water quenching. Finally, specimens were cut through the longitudinal direction (rolling direction) for metallographic purposes to investigate the evolutions of the microstructure. Optical microscopy (Meiji Techno IM7200) and scanning electron microscopy (SEM, LEO 1455 VP) were used to monitor the microstructural changes. The grain boundaries were revealed by electroetching in a 60% HNO₃ and 40% distilled water solution at 2.2 V.

The average grain sizes were determined based on the standard linear intercept method according to ASTM E112 [12]. That was done by a MIP4 software. Tensile tests were performed at room temperature according to the ASTM A356 standard using a tensile machine (SANTAM, STM150) at a strain rate of 0.003 s⁻¹. The tensile specimens were provided in the rolling direction using a wire cut machine.

The hardness of the specimens was measured by Vickers method by applying a 30 kg force. X-ray diffraction was applied using an X'Pert Pro MPD diffractometer with Cu-Kα radiation (in RD-TD direction). In addition, to calculate the volume fraction of strain-induced martensite, a feritscope (Fischer MP30) was used. The actual martensite content was determined using the following equation [6]:

$$\text{vol\% martensite} = 1.75 \times \text{Feritscope reading} \quad (1)$$

3. Results and Discussion

3.1. Microstructural evolutions during cold-rolling and annealing

Fig. 1(a) shows the optical micrograph of the as-received material, where steel consists of the austenite phase (97%) and delta ferrite (3%). The delta-ferrite phase, shown as a dark phase in Fig. 1(a), was probably formed in the early stages of solidification. The average

grain size of the austenite in the as-received specimen is 80±3 μm. Fig. 1(b) depicts the microstructure of cold-rolled specimen after a 90% thickness reduction. As is observed, the austenite grains are elongated along with a rolling direction. Moreover, according to the feritscope result, the volume fraction of the strain-induced martensite reaches 1.5% after 90% thickness reduction. In fact, 309S stainless steel contains stable austenite phase which is resistant towards the martensitic transformation during plastic deformation at room temperature. The XRD patterns of the as-received and deformed specimens are shown in Fig. 1(c) which confirms the presence of delta-ferrite or martensite phase.

The microstructure of 90% cold-rolled specimen after annealing at 700, 800, 900, and 1000°C for 3 min is shown in Fig. 2. As is observed in Fig. 2(a), annealing

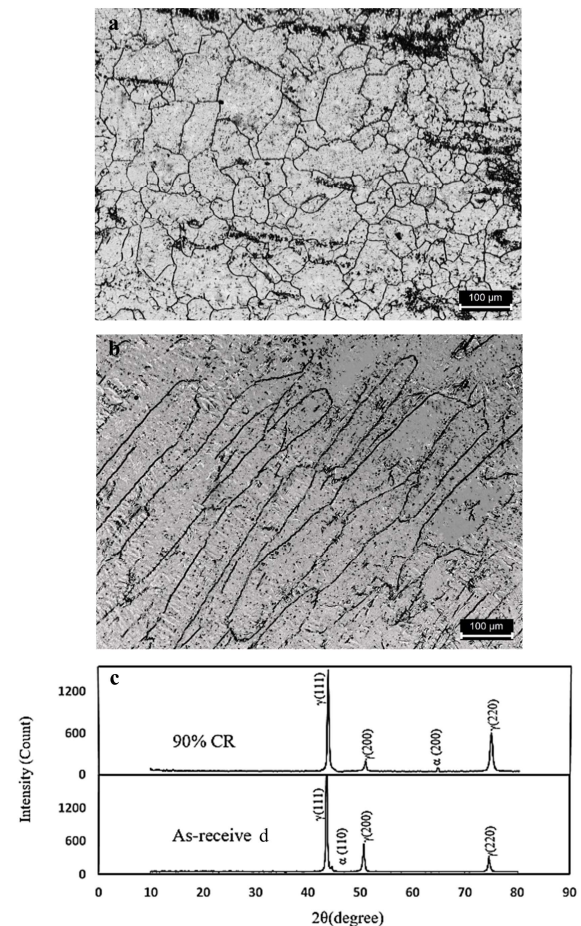


Fig. 1. (a) and (b) optical micrographs of as-received and 90% cold-rolled specimens, respectively, (c) XRD patterns of the as-received and 90% cold-rolled specimens.

at 700°C results in partial recrystallization along with considerable elongated grains which confirms that recovery is the main mechanism at 700°C for 3 min. By increasing the annealing temperature up to 800 and 900°C (Figs. 2(c) and 2(d)), the volume fraction of new fine equiaxed grains increased due to the recrystallization

phenomenon. Indeed, homogeneity of grains in terms of shape and size augmented by rising annealing temperature from 700 to 800, and 900°C. Finally, according to Fig. 2(f), an equiaxed microstructure is obtained after annealing at 1000°C for 3 min. Furthermore, grain size at 1000°C rose in comparison with

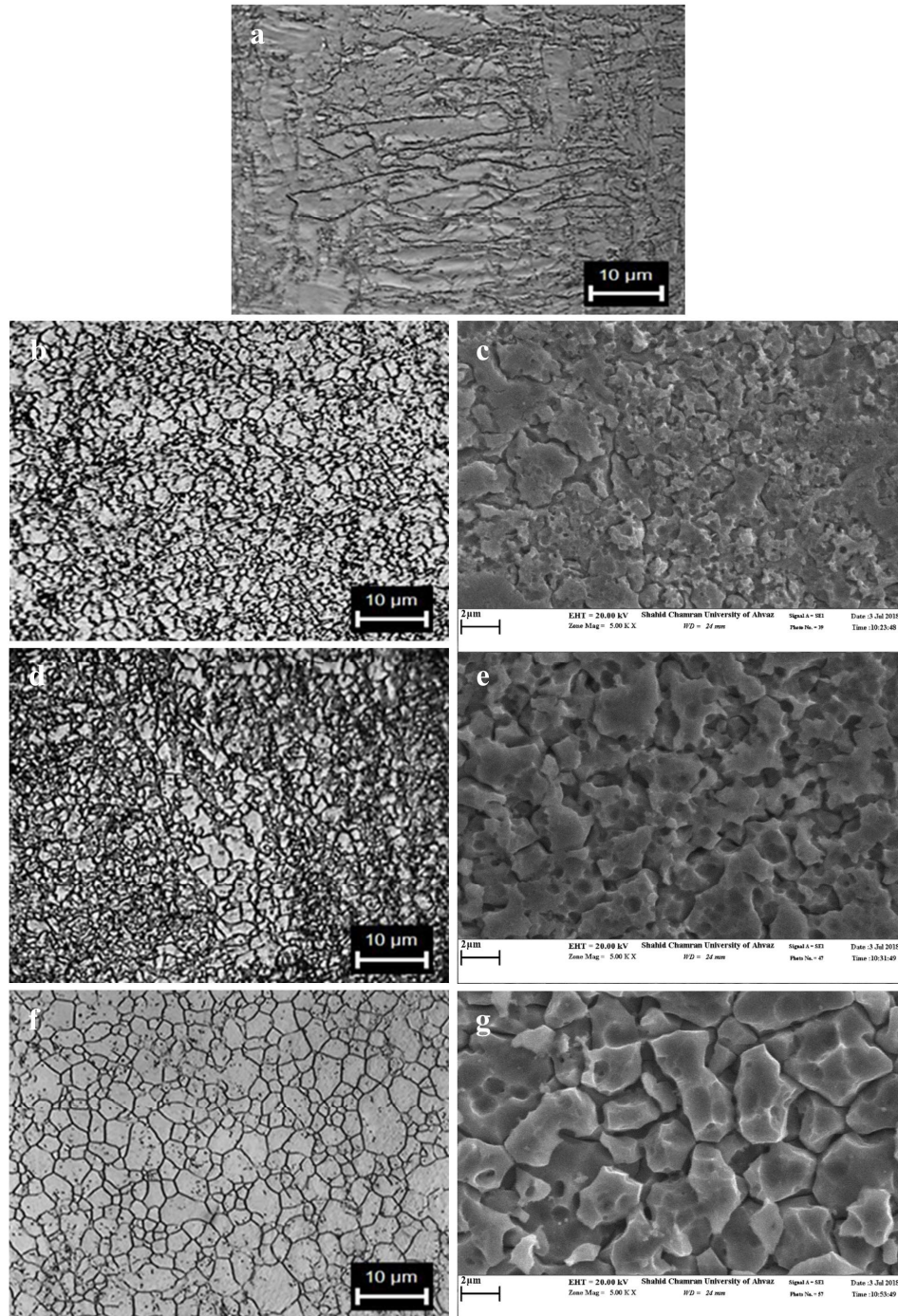


Fig. 2. OM and SEM microstructures of 90% cold-rolled specimens after annealing for 3 min: (a) at 700°C, (b) and (c) at 800°C, (d) and (e) at 900°C, (f) and (g) at 1000°C.

annealing at 800 and 900°C temperatures. The former observation confirms that normal grain growth is the prevailing mechanism at 1000°C. It should be mentioned that according to the feritscope result, the strain-induced martensite reverts to austenite during annealing. However, due to low volume fraction of the martensite (1.5%) in cold-rolled material, the effect of reversion of the martensite to austenite on the annealed microstructure is negligible.

Fig. 3 and Fig. 4 display SEM microstructures of

cold-rolled specimens after annealing at different temperatures for 10 and 20 min, respectively. As is observed in those figures, the shape of the grains is equiaxed which is a good signature of complete recrystallization after annealing for longer times. In addition, the average grain size of austenite is increased by rising the annealing temperature and time.

The variations of austenite grain size after cold-rolling and annealing for different times and temperatures are shown in Fig. 5. A uniform fine austenite

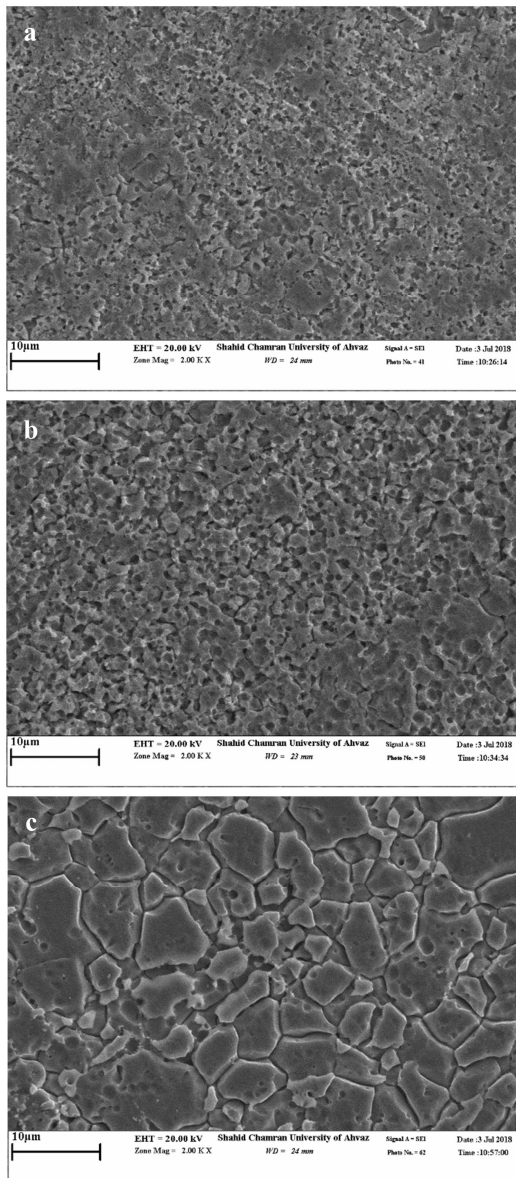


Fig. 3. SEM microstructures of 90% cold-rolled specimens after annealing for 10 min at: (a) 800°C, (b) 900°C, (c) 1000°C.

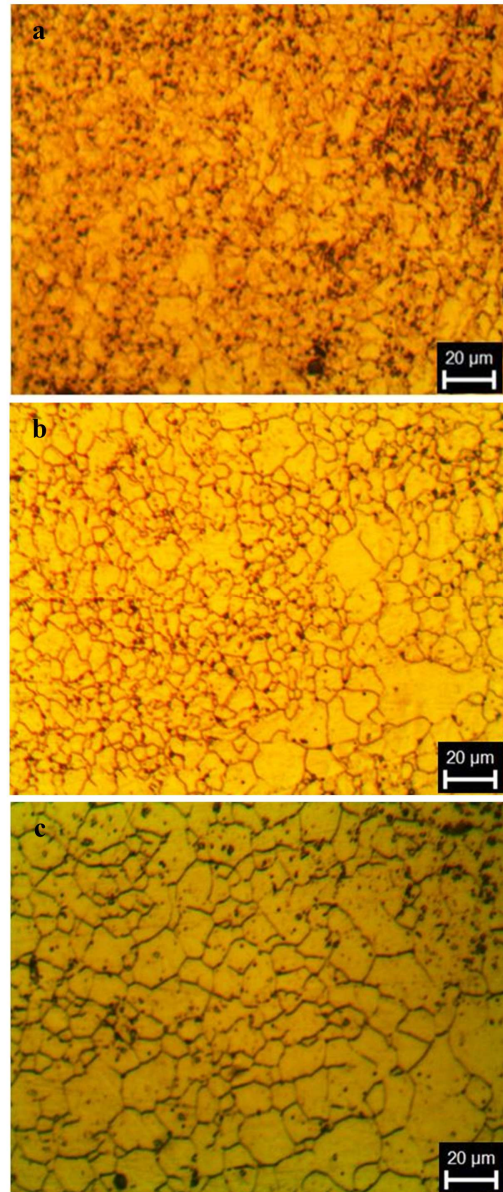


Fig. 4. OM microstructures of 90% cold-rolled specimens after annealing for 20 min at: (a) 800°C, (b) 900°C, (c) 1000°C.

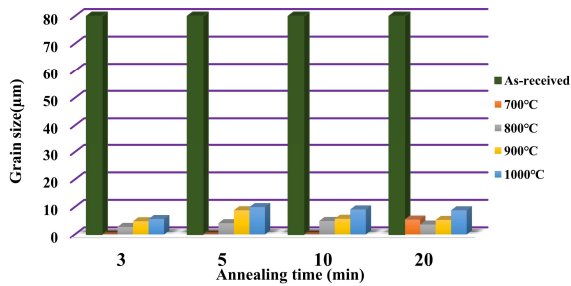


Fig. 5. Variations of grain size after cold-rolling and annealing treatments.

grain with average grain size of $2.74 \pm 0.5 \mu\text{m}$ is obtained after annealing at 800°C for 3 min. By increasing the annealing temperature to 1000°C , the average grain size is increased to $5 \pm 1 \mu\text{m}$. When compared to the grain size of the as-received specimen ($80 \pm 3 \mu\text{m}$), a significant grain refinement was achieved after the cold-rolling and annealing process. The observed grain refinement is caused due to the primary recrystallization of the austenite phase, not the martensite reversion to austenite. It is expected that the observed grain refinement improves the mechanical properties of 309S steel, which will be discussed in the following section.

Fig. 6 shows the XRD patterns of 90% cold-rolled specimens after annealing at 700, 800, 900, and 1000°C for 3 min. As is seen in Fig. 6, most of the microstructure consisted of an austenite phase and a very less delta-ferrite (according to feritscope 1.2%) that remained in the material after annealing treatments.

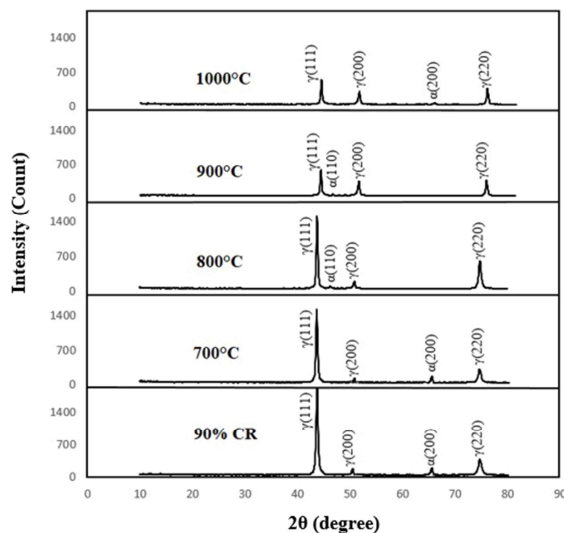


Fig. 6. XRD patterns of a 90% cold-rolled specimen after annealing at 700, 800, 900, 1000°C for 3 min.

Hence, microstructural evolutions during annealing of a cold-rolled AISI 309S are reversions of strain-induced martensite to austenite which was negligible in current work followed by the primary recrystallization of the retained austenite, and the grain growth by increasing annealing time or temperature. Indeed, two distinct stages of recrystallization and grain growth are identified in the annealing behavior of 309S steel, while annealing investigations of other austenitic stainless steels such as 316L and 304 encompass three stages [6,8]. The martensite reversion to austenite is a dominant stage in 316L, 304, 301, 321 austenitic stainless steels.

3.2. Effect of cold-rolling and annealing on the mechanical properties

Under uniaxial tensile condition, plastic deformation of 309S stainless steel is accompanied by significant strain hardening. The quantitative analysis shows that the average grain size decreases from about $80 \mu\text{m}$ in the as-received material to $2.74 \mu\text{m}$ in the annealing phase at 800°C for 3 min. Recrystallization generally proceeds through the nucleation of new grains and the subsequent grain boundary migration that consumes the prior high stored energy deformed microstructure [24]. Variations of Vickers hardness of annealed specimens at 700, 800, 900, and 1000°C for 3 and 20 min are shown in Fig. 7. According to Fig. 7(a), increasing the annealing temperature from 700 to 1000°C results in decreasing hardness value from 396 ± 3 to 215 ± 3 . As mentioned in the previous section, after annealing at 700°C , austenite grains are still elongated, and the recovery process was dominant. The elongated grains might contain high density of dislocation and that is why the hardness value of annealed specimen at 700°C is the highest among the other annealing temperatures. By increasing the annealing temperature from 700 to 800°C and 800 to 1000°C , the mechanism of restoration phenomenon is changed from recovery to recrystallization and from recrystallization to grain growth, respectively. Hence, it is expected that the steel experiences a softening behavior when annealing temperature is approached to 1000°C . The former trend was also observed for the annealed specimens for 20 min (Fig. 7(b)).

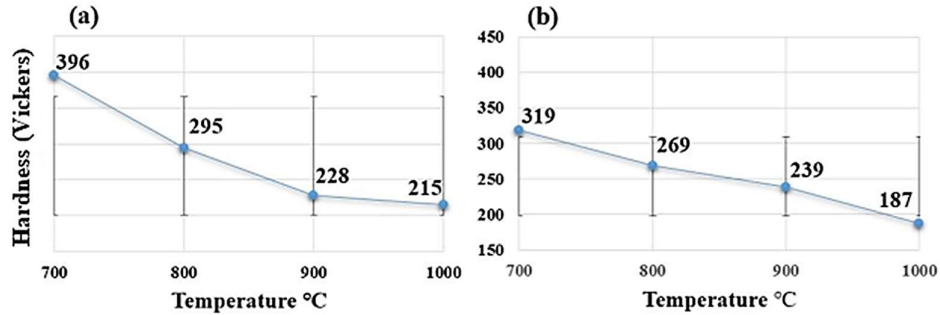


Fig. 7. Variations of Vickers hardness of annealed specimens at different temperatures for: (a) 3 min and (b) 20 min.

Fig. 8 depicts the variations caused by Vickers hardness before and after annealing treatments at 700, 800, 900 and 1000°C for different times. As is seen in Fig. 8, the hardness values of the as-received and 90% cold-rolled specimens are 225 ± 3 and 416 ± 3 , respectively. It can be concluded that the hardness values of all annealed specimens are higher and lower than the as-received and cold-rolled specimens, respectively. The annealed specimen after 90% thickness reduction consisted of elongated grains with a high density of dislocation within grains. Therefore, it is expected that the cold-rolled specimen shows higher hardness compared to annealed specimens.

Fig. 9 plots the variations of grain size and hardness versus annealing temperatures for 3 min. Annealed specimens at all temperatures depicted a smaller grain size in contrast to the as-received specimen due to grain

refinement because of recrystallization. The grain size of annealed specimen increased by rising the annealing temperature from 800°C to 1000°C due to grain growth mechanism. In addition, the annealed specimen at 800°C has the smallest and the highest grain size and hardness, respectively.

Fig. 10 displays engineering stress-strain curves of 90% cold-rolled specimens after annealing at different temperatures for 3 to 10 min. The stress-strain curves of specimens were obtained at room temperature and yield stress of (YS) specimens were achieved according to the offset method.

As is observed in Fig. 10, as-received and annealed specimens show continuous yielding followed by strain hardening up to the final fracture. The as-received material depicts the lowest yield stress (155 ± 4 MPa) and the highest elongation to fracture (107%) compared to

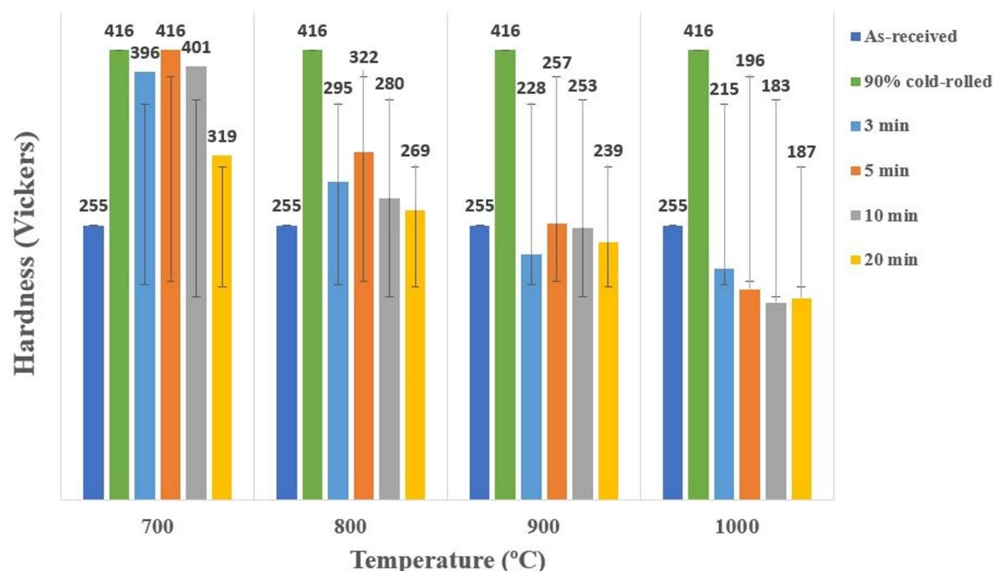


Fig. 8. Variations of Vickers hardness before and after annealing treatments at 700, 800, 900 and 1000°C for different times.

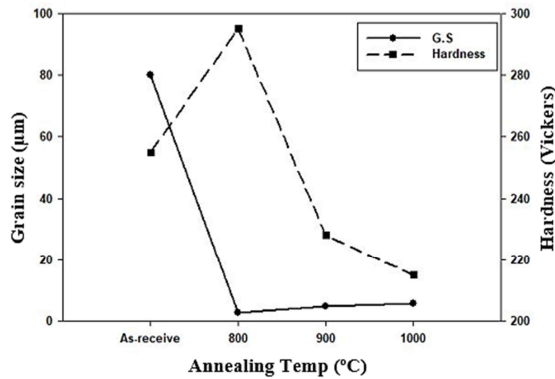


Fig. 9. Variations of hardness and grain size of annealed specimens at different temperatures for 3 min.

all annealed specimens. The yield stress, ultimate tensile stress (UTS), and strain of failure of annealed specimens at different temperatures for 3 and 10 min are shown in Tables 2 and 3, respectively. The YS of as-received specimen was increased from 155 to 803, 790, 750, and 620 MPa after annealing at 700, 800, 900, and 1000°C, respectively. In fact, the YS of as-received specimen at 80% improved after annealing to 800°C for 3 min.

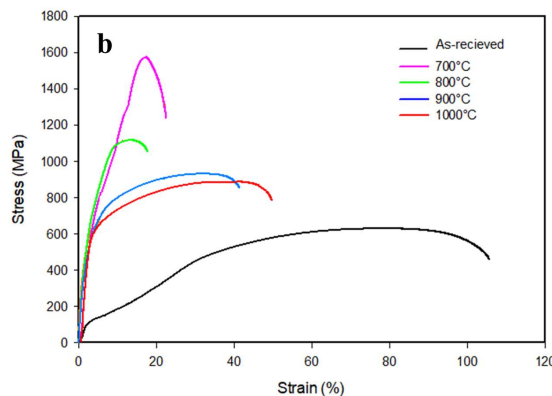
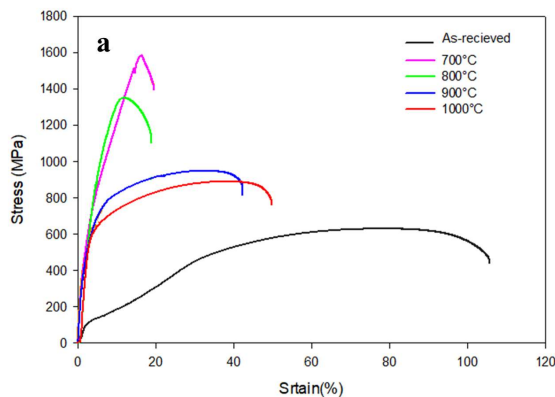


Fig. 10. Engineering stress-strain curves of annealed specimens at different temperatures for: (a) 3 min, and (b) 10 min.

Table 2. The yield stress (YS), ultimate tensile stress (UTS), and strain of failure of annealed specimens at temperature range of 700-1000°C for 3 min

Specimen	YS (MPa)	UTS (MPa)	Strain of failure (%)
As-received	155	629	107
700°C	803	1584	20
800°C	790	1349	19
900°C	750	948	40
1000°C	620	898	49

Table 3. The yield stress (YS), ultimate tensile stress (UTS), and strain of failure of annealed specimens at temperature range of 700-1000°C for 10 min.

Specimen	YS (MPa)	UTS (MPa)	Strain of failure (%)
As-received	155	629	107
700°C	750	1574	21
800°C	704	1116	17
900°C	610	931	41
1000°C	601	890	50

Another issue is related to the effect of annealing temperatures on the mechanical behavior of annealed specimens. By increasing annealing temperatures from 700 to 1000°C, flow stress and elongation to fracture are decreased and increased, respectively. In addition, Tables 2 and 3 depict that in the case of constant temperatures, as the annealing time increases from 3 to 10 min, the YS decreases. However, it is evident that the strain of failure would improve. The latter observation is attributed to increasing the grain size by increasing the annealing time and its effect on the Hall-Petch equation and grain boundary strengthening. The improvement of mechanical properties in current work was also observed in [25].

4. Conclusion

In the present study, the cold-rolling and annealing behavior of a 309S austenitic stainless steel was studied. It was detected that very less strain-induced martensitic transformation formed after 90% thickness reduction. During annealing, two stages of recrystallization of the retained austenite, and grain growth were identified. These stages controlled the microstructures and mechanical properties of the material. It was found that the slow kinetics of static recrystallization at a low annealing temperature of 700°C inhibited the formation

of an equiaxed microstructure and elongated grains were observed. However, with the increase of the annealing temperature to 800°C for 3 min, the presence of the recrystallized grains was clear and the average grain size reduced to 2.74 μm . Higher annealing temperatures of 900, and 1000°C resulted in the growth of grains. The present thermomechanical treatments improved the yield stress of material by 40% in comparison with the as-received condition.

Acknowledgements

The Shahid Chamran University of Ahvaz financially supported this research with grant number SCU.EM1400.30796.

Conflict of Interests

The authors declare that they have no conflict of interest.

5. References

- [1] J.A. Lichtenfeld, C.J. Van Tyne, M.C. Mataya, Effect of strain rate on stress-strain behavior of alloy 309 and 304L austenitic stainless steel, *Metallurgical and Materials Transactions A*, 37(1) (2006) 147-161.
- [2] W. Ye, Y. Li, F. Wang, Effects of nanocrystallization on the corrosion behavior of 309 stainless steel, *Electrochimica Acta*, 51(21) (2006) 4426-4432.
- [3] R. Singh, S. Goel, R. Verma, R. Jayaganthan, A. Kumar, Mechanical behaviour of 304 austenitic stainless steel processed by room temperature rolling, *Materials Science and Engineering*, 330(1) (2018) 012017.
- [4] H. Kotan, K.A. Darling, A study of microstructural evolution of Fe-18Cr-8Ni, Fe-17Cr-12Ni, and Fe-20Cr-25Ni stainless steels after mechanical alloying and annealing, *Materials Characterization*, 138 (2018) 186-194.
- [5] A.A. Tihamiyu, J.A. Szpunar, A.G. Odeshi, I. Oguocha, M. Eskandari, Development of ultra-fine-grained structure in AISI 321 austenitic stainless steel, *Metallurgical and Materials Transactions A*, 48(12) (2017) 5990-6012.
- [6] M. Karimi, A. Najafizadeh, A. Kermanpur, M. Eskandari, Effect of martensite to austenite reversion on the formation of nano/submicron grained AISI 301 stainless steel, *Materials Characterization*, 60(11) (2009) 1220-1223.
- [7] A. Rezaei, A. Najafizadeh, A. Kermanpur, M. Moalemi, Analysis of microstructural evolution of AISI 201L stainless steel, during advanced thermomechanical processing, Steel Symposium 89, Isfahan Steel Company, Isfahan, Iran, (2011).
- [8] M. Eskandari, A. Najafizadeh, A. Kermanpur, Effect of strain-induced martensite on the formation of nanocrystalline 316L stainless steel after cold rolling and annealing, *Materials Science and Engineering: A*, 519(1-2) (2009) 46-50
- [9] D.M. Xu, G.Q. Li, X.L. Wan, R.D.K. Misra, X.G. Zhang, G. Xu, K.M. Wu, The effect of annealing on the microstructural evolution and mechanical properties in phase reversed 316LN austenitic stainless steel, *Materials Science and Engineering: A*, 720 (2018) 36-48.
- [10] R.D.K. Misra, J.S. Shah, S. Mali, P.K.C. Venkata Surya, M.C. Somani, L.P. Karjalainen, Phase reversion induced nanograined austenitic stainless steels: microstructure, reversion and deformation mechanisms, *Materials Science and Technology*, 29(10) (2013) 1185-1192.
- [11] P. Behjati, A. Kermanpur, A. Najafizadeh, H.S. Baghbadorani, Effect of annealing temperature on nano/ultrafine grain of Ni-free austenitic stainless steel, *Materials Science and Engineering: A*, 592 (2014) 77-82.
- [12] ASTM E112-96, Standard test methods for determining average grain size, ASTM International, 2004.
- [13] Z. Wang, A.M. Beese, Effect of chemistry on martensitic phase transformation kinetics and resulting properties of additively manufactured stainless steel, *Acta Materialia*, 131 (2017) 410-422.
- [14] R. Song, D. Ponge, D. Raabe, J.G. Speer, D.K. Matlock, Overview of processing, microstructure and mechanical properties of ultrafine grained bcc steels, *Materials Science and Engineering: A*, 441(1-2) (2006) 1-17.
- [15] C. Donadille, R. Valle, P. Dervin, R. Penelle, Development of texture and microstructure during cold-rolling and annealing of FCC alloys: example of an austenitic stainless steel, *Acta Metallurgica*, 37(6) (1989) 1547-1571.
- [16] S.W. Yang, J.E. Spruiell, Cold-worked state and annealing behaviour of austenitic stainless steel, *Journal of Materials Science*, 17(3) (1982) 677-690.
- [17] A. Belyakov, T. Sakai, H. Miura, R. Kaibyshev, K. Tsuzaki, Continuous recrystallization in austenitic stainless steel after large strain deformation, *Acta Materialia*, 50(6) (2002) 1547-1557.
- [18] B.R. Kumar, S.K. Das, B. Mahato, A. Das, S.G. Chowdhury, Effect of large strains on grain boundary

- character distribution in AISI 304L austenitic stainless steel, *Materials Science and Engineering: A*, 454 (2007) 239-244.
- [19] F.J. Humphreys, M. Hatherly, Recrystallization and related annealing phenomena, Elsevier, 2012.
- [20] S.G. Chowdhury, S. Das, B. Ravikumar, P.K. De, Twinning-induced sluggish evolution of texture during recrystallization in AISI 316L stainless steel after cold rolling, *Metallurgical and Materials Transactions A*, 37(8) (2006) 2349-2359.
- [21] X.H. Chen, J. Lu, L. Lu, K. Lu, Tensile properties of a nanocrystalline 316L austenitic stainless steel, *Scripta Materialia*, 52(10) (2005) 1039-1044.
- [22] M. Eskandari, A. Zarei-Hanzaki, H.R. Abedi, An investigation into the room temperature mechanical properties of nanocrystalline austenitic stainless steels, *Materials & Design*, 45 (2013) 674-681.
- [23] I. Shakhova, V. Dudkoa, A. Belyakova, K. Tsuzaki, R. Kaibyshev, Effect of large strain cold rolling and subsequent annealing on microstructure and mechanical properties of an austenitic stainless steel, *Materials Science and Engineering: A*, 545 (2012) 176-186.
- [24] M.J.N.V. Prasad, M.W. Reiterer, K.S. Kumar, Microstructure and mechanical behavior of annealed MP35N alloy wire, *Materials Science and Engineering: A*, 636 (2015) 340-351.
- [25] Y.Z. Zhang, J.J. Wang, N.R. Tsoa, Tensile ductility and deformation mechanisms of a nanotwinned 316L austenitic stainless steel, *Journal of Materials Science & Technology*, 36 (2020) 65-69.